NASA/TM—2003-212183 ARL–TR–2929

U.S. ARMY
RESEARCH LABORATORY

Experimental High Temperature Characterization of a Magnetic Bearing for Turbomachinery

Gerald Montague
U.S. Army Research Laboratory, Glenn Research Center, Cleveland, Ohio

Mark Jansen
University of Toledo, Toledo, Ohio

Andrew Provenza
Glenn Research Center, Cleveland, Ohio

Alan Palazzolo
Texas A&M University, College Station, Texas

Ralph Jansen and Ben Ebihara
University of Toledo, Toledo, Ohio

March 2003

The NASA STI Program Office . . . in Profile

Since its founding, NASA has been dedicated to the advancement of aeronautics and space science. The NASA Scientific and Technical Information (STI) Program Office plays a key part in helping NASA maintain this important role.

The NASA STI Program Office is operated by Langley Research Center, the Lead Center for NASA's scientific and technical information. The NASA STI Program Office provides access to the NASA STI Database, the largest collection of aeronautical and space science STI in the world. The Program Office is also NASA's institutional mechanism for disseminating the results of its research and development activities. These results are published by NASA in the NASA STI Report Series, which includes the following report types:

- TECHNICAL PUBLICATION. Reports of completed research or a major significant phase of research that present the results of NASA programs and include extensive data or theoretical analysis. Includes compilations of significant scientific and technical data and information deemed to be of continuing reference value. NASA's counterpart of peer-reviewed formal professional papers but has less stringent limitations on manuscript length and extent of graphic presentations.

- TECHNICAL MEMORANDUM. Scientific and technical findings that are preliminary or of specialized interest, e.g., quick release reports, working papers, and bibliographies that contain minimal annotation. Does not contain extensive analysis.

- CONTRACTOR REPORT. Scientific and technical findings by NASA-sponsored contractors and grantees.

- CONFERENCE PUBLICATION. Collected papers from scientific and technical conferences, symposia, seminars, or other meetings sponsored or cosponsored by NASA.

- SPECIAL PUBLICATION. Scientific, technical, or historical information from NASA programs, projects, and missions, often concerned with subjects having substantial public interest.

- TECHNICAL TRANSLATION. English-language translations of foreign scientific and technical material pertinent to NASA's mission.

Specialized services that complement the STI Program Office's diverse offerings include creating custom thesauri, building customized databases, organizing and publishing research results . . . even providing videos.

For more information about the NASA STI Program Office, see the following:

- Access the NASA STI Program Home Page at ***http://www.sti.nasa.gov***

- E-mail your question via the Internet to help@sti.nasa.gov

- Fax your question to the NASA Access Help Desk at 301–621–0134

- Telephone the NASA Access Help Desk at 301–621–0390

- Write to:
  NASA Access Help Desk
  NASA Center for AeroSpace Information
  7121 Standard Drive
  Hanover, MD 21076

NASA/TM—2003-212183

ARL–TR–2929

Experimental High Temperature Characterization of a Magnetic Bearing for Turbomachinery

Gerald Montague
U.S. Army Research Laboratory, Glenn Research Center, Cleveland, Ohio

Mark Jansen
University of Toledo, Toledo, Ohio

Andrew Provenza
Glenn Research Center, Cleveland, Ohio

Alan Palazzolo
Texas A&M University, College Station, Texas

Ralph Jansen and Ben Ebihara
University of Toledo, Toledo, Ohio

Prepared for the
59th Annual Forum and Technology Display
sponsored by the American Helicopter Society
Phoenix, Arizona, May 6–8, 2003

National Aeronautics and
Space Administration

Glenn Research Center

March 2003

Acknowledgments

This research was funded by NASA Glenn Research Center's Smart Efficient Components program (SEC), which is managed by Bob Corrigan. The authors would like to thank Peter Kascak (University of Toledo) for his assistance in the power measurement, Julie Roden (Analex, Corp.) for her thermal expansion analysis, John Poles (NASA Glenn) for his significant electrical contributions, and Tim Czaruk (QSS Group, Inc.) for test support. The authors would also like to recognize Gerald Brown and Albert Kascak (NASA Glenn) for their expert guidance and review. Final recognition is for Texas A&M students Randy Tucker, Jason Preuss, and Andrew Hunt who designed and constructed the high temperature coils used in this magnetic bearing.

This report is a formal draft or working paper, intended to solicit comments and ideas from a technical peer group.

The Propulsion and Power Program at NASA Glenn Research Center sponsored this work.

Available from

NASA Center for Aerospace Information
7121 Standard Drive
Hanover, MD 21076

National Technical Information Service
5285 Port Royal Road
Springfield, VA 22100

Available electronically at http://gltrs.grc.nasa.gov

Experimental High Temperature Characterization of a Magnetic Bearing for Turbomachinery

Gerald Montague
U.S. Army Research Laboratory
Glenn Research Center
Cleveland, Ohio 44135

Mark Jansen
University of Toledo
Toledo, Ohio 43606

Andrew Provenza
National Aeronautics and Space Administration
Glenn Research Center
Cleveland, Ohio 44135

Alan Palazzolo
Texas A&M University
College Station, Texas 77843

Ralph Jansen and Ben Ebihara
University of Toledo
Toledo, Ohio 43606

ABSTRACT

Open loop, experimental force and power measurements of a radial, redundant-axis, magnetic bearing at temperatures to 1000 °F (538 °C) and rotor speeds to 15,000 RPM along with theoretical temperature and force models are presented in this paper. The experimentally measured force produced by a single C-core using 22A was 600 lb. (2.67 kN) at room temperature and 380 lb. (1.69 kN) at 1000 °F (538 °C). These values were compared with force predictions based on a 1D magnetic circuit analysis and a thermal analysis of gap growth as a function of temperature. Tests under rotating conditions showed that rotor speed has a negligible effect on the bearing's load capacity. One C-core required approximately 340 W of power to generate 190 lb. (8.45 kN) of magnetic force at 1000 °F (538 °C); however the magnetic air gap was much larger than at room temperature. The data presented is after the bearing had already operated six thermal cycles and eleven total (not consecutive) hours at 1000 °F (538 °C).

INTRODUCTION

The gas turbine industry has a continued vested interest in improving engine performance and reducing net operating and maintenance costs. These goals are being realized because of advancements in aeroelasticity, materials, computational tools such as CFD, and engine simulations. These advancements also aid in increasing engine thrust-to-weight ratios, pressure ratios, specific fuel consumption, and overall reliability through higher efficiency engine operation at higher rotational speeds and higher temperatures.

Rolling element bearings and squeeze film dampers are currently used to support gas turbine engine rotors. These types of bearings are limited in temperature (<260 °C) and speed (< 2.5 million DN) and require both cooling air and a lubrication system. Rolling element bearings in gas turbines are being pushed to their limits and new bearing technologies must be developed to take full advantage of other aforementioned advancements.

Magnetic bearings are well suited to operate at elevated temperature, higher rotational speeds, and extreme altitudes (thin air atmosphere) and are a promising solution to these current limitations.

Magnetic bearing technology is being developed worldwide and is considered an enabling technology for new, hotter engine designs. Xu, Wang, and Schweitzer developed two high temperature magnetic bearing test rigs, a one degree of freedom and a five degree of freedom rig to demonstrate operation of a magnetic bearing at high temperature [1]. A 1,500 hour test of a magnetic bearing for a 176 lb (80 kg), 12,000 RPM blower rotor operating at 750 °F (399 °C) was completed by Ohsawa et al. [2]. High temperature magnetic properties of candidate magnetic materials were investigated in the sixties by Kueser et al., [3] and recently by Kondoleon and Kelleher [4]. This paper advances the wafer test specimen results from [3] and [4] to a laminated c-core magnet. Magnetic bearings in gas turbine engines would eliminate lubrication analysis, leaks, spills, contamination, and unnecessary maintenance due to faulty chip detection. The magnetic bearing could provide health monitoring and adaptively modify the rotor support to actively respond to transients such as hard aircraft landings and sudden imbalances.

Magnetic bearings will enable engine designers to take full advantage of other technological advancements in turbine engine components by allowing rotor components to spin at higher speeds and at higher temperatures. As a result, turbine and compressor spools can be designed with higher operating temperatures and with significantly larger, faster, stiffer, highly damped rotors. Mekhiche developed a high temperature magnetic bearing system that is described from design through testing in [5]. This paper performs similar test using a different approach and shows detailed results and interpretation.

The 3rd generation high temperature, high load magnetic bearing, developed at the NASA Glenn Research Center, was first characterized at room temperature (R.T.) up to 20,000 RPM. It is capable of producing over 1,000 lb (4.5 kN) of loading per magnetic axis at R.T. and at speed. R.T. data for this bearing is presented in [6].

Data presented in this paper characterizes the 3rd generation bearing at temperatures up to 1,000 °F (537 °C). Bearing force as a function of current, temperature, and speeds to 15,000 RPM is shown. In addition, bearing power consumption measurements taken at several applied current and temperatures are presented.

TEST FACILITY

FACILITY DESCRIPTION

The high temperature magnetic bearing test facility is shown in Figure 1. The structural support can accommodate thrust and radial bearings up to 9.0 in (22.8 cm) diameter with a maximum axial loading of 5,000 lb (22.3 kN) and a maximum radial loading of 2,500 lb (11.1 kN). The test facility has been configured a number of different ways [6, 7].

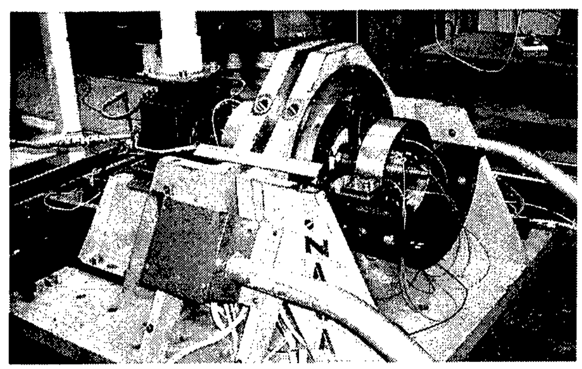

Figure 1 – High temperature magnetic bearing test facility at NASA Glenn Research Center.

The current configuration can be seen in Figure 2. The magnetic bearing is located at the center of gravity of the 2.98 in (75 mm) diameter rotor that weighs 17 lbs (7.7 kg). The 8.0 in (203 mm) stator weighs 52 lbs (23.5 kg). A 0.022 in (0.56 mm) radial air gap exists between the stator poles and the rotor at R.T. The rotor has interchangeable sleeves on each end that interface it with the support bearings, which, for these tests, are high-speed, grease packed, duplex ball bearings. For this configuration, the rotor was fitted with zero clearance sleeves so it

was supported on the ball bearings at both ends. This was done so that forces exerted by the magnetic bearing could be easily and directly measured outside the hot section at the support bearing locations. The outboard sleeve can be replaced with a positive clearance sleeve so that the magnetic bearing can support the rotor. An air turbine drives the rotor.

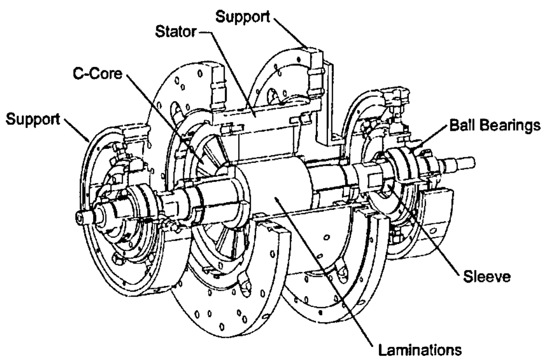

Figure 2 – Third generation high temperature magnetic bearing facility.

The magnetic bearing stator is an isolated C-core, 12-pole, heteropolar design and is described in detail in [8]. The stator has a width of 3.4 in. (76.1 mm). Each C-core is wrapped with two coils and each coil has 52 turns of specially insulated and potted wire. The coil packing factor is 0.67.

Power to the magnetic bearing is provided through six tri-state, pulse width modulated (PWM) amplifiers. These components are passively filtered to remove high frequency amplifier noise that results from amplifier switching and to reduce EMI emissions from the bearing coils that interfere the eddy current position sensor's signal.

Heat is supplied to the bearing through three, 3 kW band heaters wrapped around the stator OD (Figure 2). Ground Fault Circuit Interrupts (GFCI) has been incorporated into the heating system and the PWM amplifier circuits to protect the hardware and for safeguarding personnel. The facility is fully described in [8]. Figure 3 shows the facility at 1,000 °F (538 °C) with the stator glowing "orange" hot.

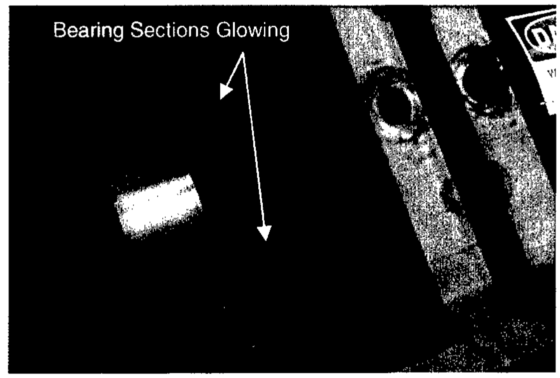

Figure 3 - Magnetic bearing at 1000 °F (540 °C).

SENSORS

The facility is equipped with several different types of sensors that monitor load, temperature, rotor positions, speed, and electric current.

High load, high bandwidth, piezoelectric load cells with accuracy of ±0.3 lb (±1.5 N), support the inboard and outboard rolling element bearings (Figure 4). These load cells are capable of measuring loads up to 1,688 lb (7.5 kN) at 200 kHz and have a maximum operating temperature of 385 °F (196 °C). Two load cells are aligned along each of the three magnetic bearing axes on both support ball bearings for a total of 12 load cells. Each load cell was set with a preload of ~250 lb (1.1 kN). This preload value supplied symmetric structural rotor support, put the critical speed out of the operating range, and established a large dynamic range. The preload was electronically zeroed during testing.

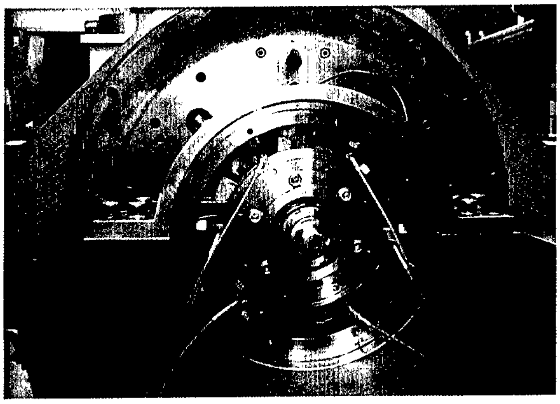

Figure 4 – Six load cells supporting the outboard duplex ball bearing.

Temperatures are recorded at several locations within the test rig. Each side face of the stator has three thermocouples mounted on it. Each set of support ball bearings is also equipped with a thermocouple. A handheld infrared thermometer is also used periodically to gather additional thermal information about the shaft temperatures during rotation.

Commercially-available, high-temperature, eddy current displacement probes are used just outside the stator on both sides of the magnetic bearing to monitor rotor position. Each side has four probes (X+, X-, Y+, Y-) for a total of eight probes. The probes are capable of 30 μin (0.0012 mm) accuracy and are temperature compensated for the 1,000 °F (538 °C) environment.

Other sensors include: an eddy current displacement probe used to measure rotor RPM and phase, magneto-resistive current sensors to measure C-core currents, and temperature/redundant RPM sensors in the air turbine.

DATA ACQUISITION

The facility data acquisition system is capable of capturing data at rates up to 15,000 samples per second per channel. Data is recorded for inboard and outboard bearing loads, support bearing and stator temperatures, X and Y axis displacements, rotor speed, and bearing C-core currents. Data is displayed in real time and can be saved directly into spreadsheet format.

EXPERIMENTAL

For the tests reported in this paper, the shaft was mounted on zero clearance ball bearing supports so the load exerted by the magnetic bearing C-cores on the rotor, could be measured outside of the hot section of the test facility.

The maximum load capacity for the bearing was determined by calculating the vector sum of the forces produced by any three C-cores along the middle core's centroid axis. The primary force component was generated by the C-core inline with that axis. Each C-core adjacent to the primary C-core also contributed a component of force in the direction of the axis (Figure 5). For example, the total load in the C-core #3 direction is the sum of the F_2 and the cosine of F_1 and F_3. The sine components of the F_1 and F_3 cancel each other out. This axis is referred to as the #2-3-4 magnetic axis.

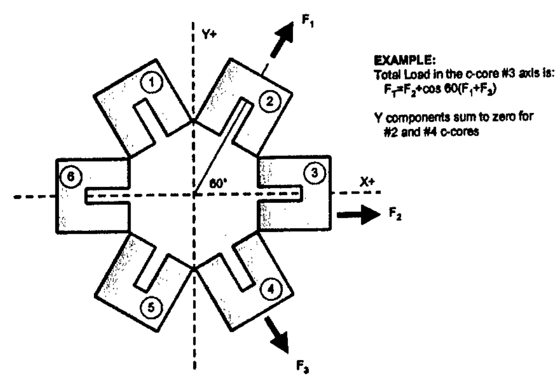

Figure 5 – Total load on each magnetic axis is a vector sum of the force from three C-cores.

MAXIMUM FORCE PRODUCE BY A SINGLE CORE AS A FUNCTION OF TEMPERATURE

Recorded data sets of load capacity vs. temperature indicate the maximum load capacity of a single core and the current level where saturation is reached. For these tests, C-core #1 was attached directly to a high power DC supply (100 V, 40 A) and load was measured while current was increased. This

was done at several different temperatures. "Saturation level" is defined as the point at which the rotor and stator laminations approach a permeability equivalent to that of air. This is the point where lamination material can not carry any additional magnetic flux.

Results are shown in Figure 6. Clearly, the data shows that force starts to become nonlinear and saturation sets in at around 17 A for each temperature set. This data also shows that the load capacity decreases by 36% at 22 A between R.T. and 1000 °F (538 °C). In [7], Minihan, et al., showed a force capacity degradation of about 33% between R.T. and 1,000 °F (538 °C) for the 2nd generation high temperature magnetic bearing. In both cases the heat source was on the outside of the stator creating a thermal gradient between the rotor and stator. By the conclusion of this paper, the data will show the reduction in force is due to an increase in the air gap due to thermal expansion and not due to lamination material properties.

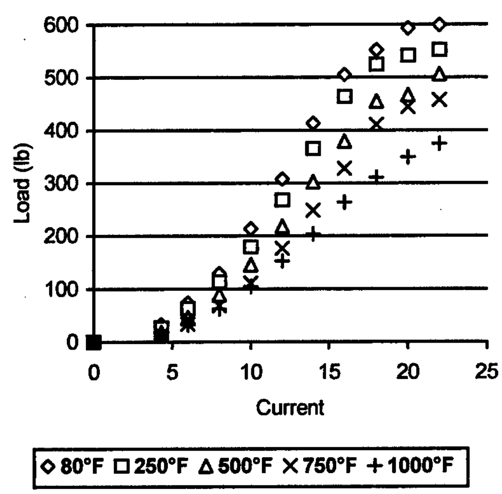

Figure 6 – Maximum load and saturation level for C-core #1 as a function of temperature.

INDIVIDUAL C-CORE LOAD CAPACITY AS A FUNCTION OF SPEED AND TEMPERATURE

Typical load capacity of a single C-core as a function of current, speed, and temperature is presented here. C-core #2 load capacity data from 0 to 15,000 RPM and from 80 °F (27 °C) to 1,000 °F (538 °C) are shown in Figures 7–10.

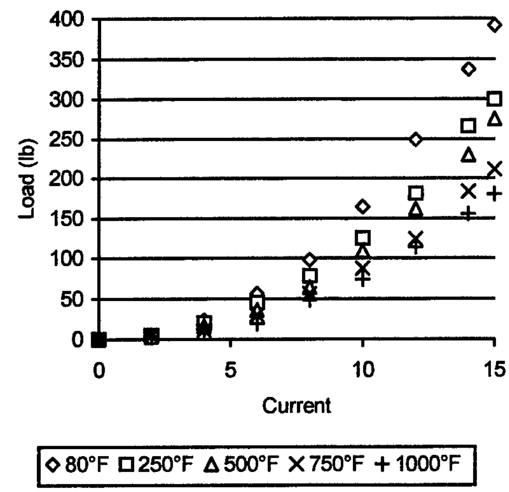

Figure 7 – Load as a function of current for C-core #2 at zero RPM.

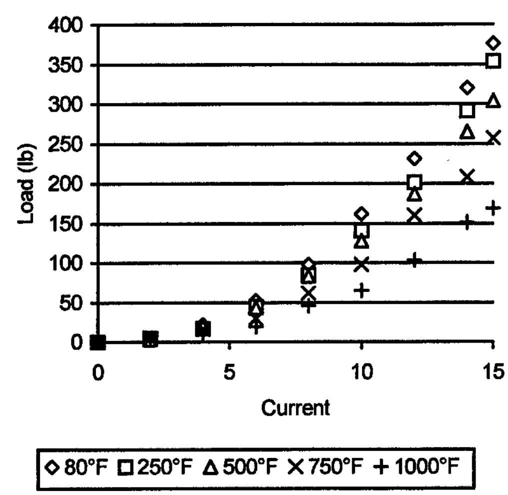

Figure 8 – Load as a function of current for C-core #2 at 5,000 RPM.

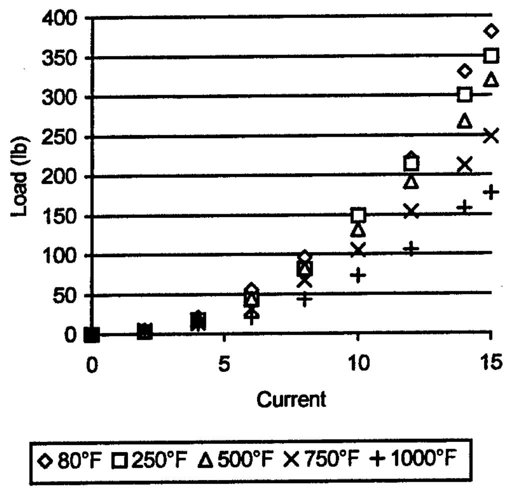

Figure 9 – Load as a function of current for C-core #2 at 10,000 RPM.

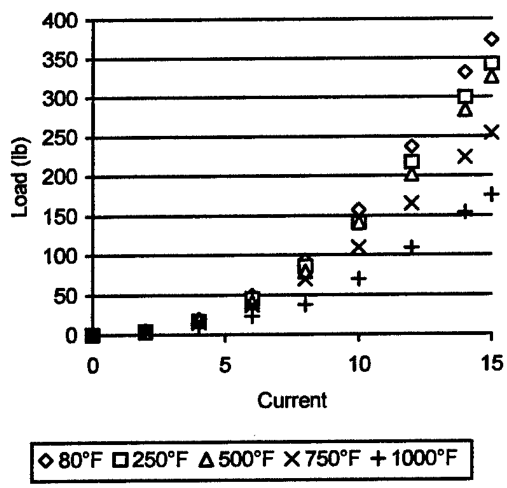

Figure 10 – Load as a function of current for C-core #2 at 15,000 RPM.

The authors recognize that there are frictional forces generated within the rolling element bearings that are not accounted for in these results. However, the bearings provide a good load path from the rotating shaft.

The option of measuring forces at the stator (Figure 12) has been tried prior to this publication. The problem with this method was that the load cells had to be in line with the stator mechanical support and an actuator system was required. This support configuration permitted stator deflection and position slip during dynamic tests.

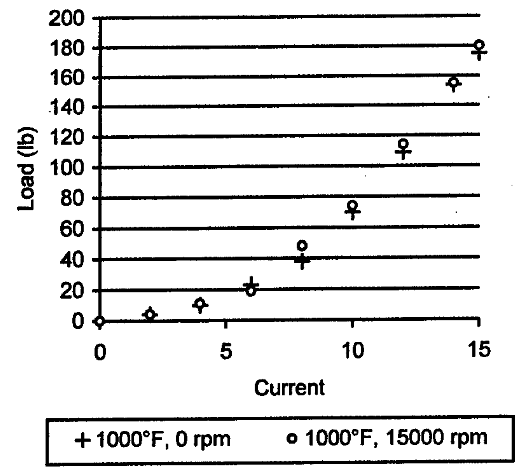

Figure 11 – Load vs. Speed comparison

As the speed increases, rotor eddy current and hysteresis losses increase. However, Figure 11 shows these losses do not affect the static load production capability of this bearing at elevated temperatures up to 15,000 rpm. These losses still have significant effects on actuator bandwidth.

For this particular C-core, a decrease in load capacity of 53% is evident at, 15 A, between R.T. and 1,000 °F (538 °C). This is a considerable amount higher than previous results have shown. Since force is proportional to the inverse square of the total air gap, small air gap changes can greatly affect bearing output for any current values. It would appear that Figures 7–10 would have shown a more favorable result if they contained data shown for C-core #1. But, it is highly likely that the test rig reached an equilibrium temperature when data was recorded for Figure 6.

These tests were performed immediately when the stator had reached the desired test point temperature. Band heaters heat the back iron of the stator and the heat travels to all other components primarily through conduction and radiation. Consequently, the rotor takes longer to heat and therefore the air gap is larger than at room temperature. In fact, air gap size is a direct function of the difference in temperature between the rotor and the stator.

Maintaining a uniform air gap for these tests is difficult. Concentricity within the rig has also been a challenge. The eight displacement sensors monitored position during all the tests to ensure the rotor did not bow or change position relative to the support stand. However, the stator was not monitored and its position may have changed slightly due to slipping, thus changing the air gap between the coils.

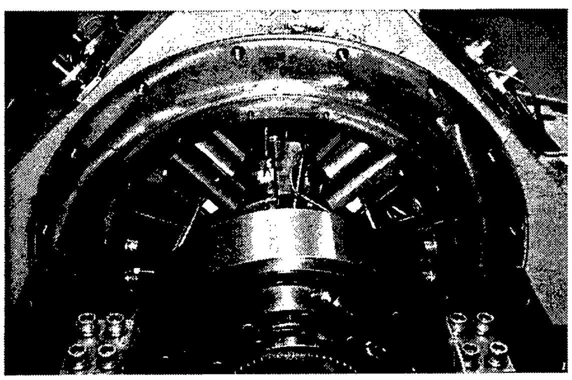

Figure 12 – Load measurements at the stator using piezoelectric actuators.

LOAD CAPACITY OF AN AXIS AS A FUNCTION OF SPEED AND TEMPERATURE

The previous tests were expanded upon to determine the load capacity of an axis. The maximum load of an axis is a function of three adjacent C-cores. The two C-cores on either side of the main axis have a contribution to the total load in that axis (Figure 4).

The results of load vs. current and temperature for zero rpm to 15,000 rpm using magnetic axis 2-3-4 are shown in Figures 13–16.

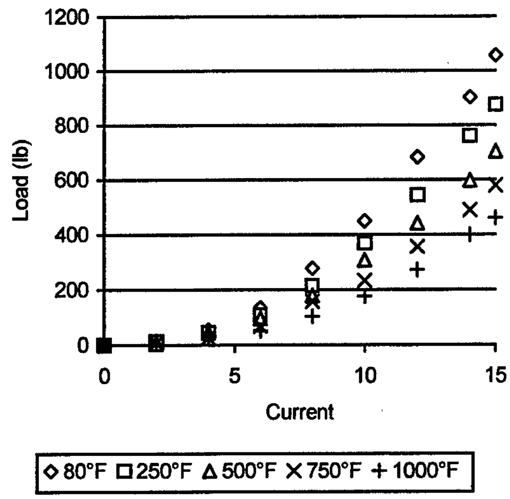

Figure 13 – Load as a function of current and temperature for the #2-3-4 magnetic axes at zero RPM.

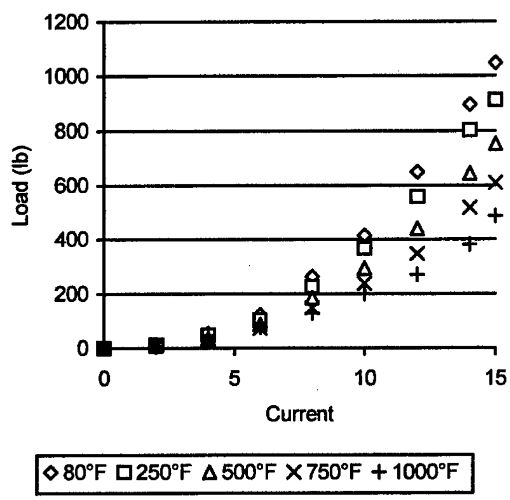

Figure 14 – Load as a function of current and temperature for the #2-3-4 magnetic axes at 5,000 RPM.

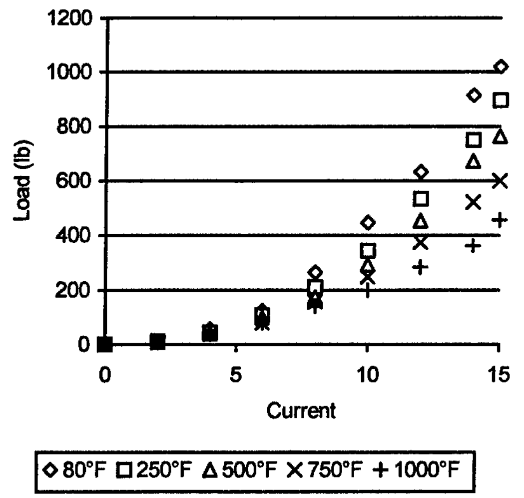

Figure 15 – Load as a function of current and temperature for the #2-3-4 magnetic axes at 10,000 RPM.

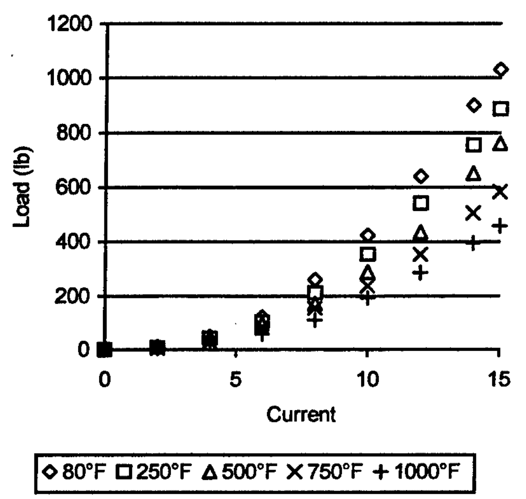

Figure 16 – Load as a function of current and temperature for the #2-3-4 magnetic axes at 15,000 RPM.

Once again, Figures 13–16, clearly show that speed does not have an effect on the load capacity of the magnetic axis at any temperature — at least to 15,000 RPM.

To confirm that the applied magnetic force was in same direction as the center C-core of that axis, the angle at which the load was applied was monitored. This was done by taking the load cell data in real-time and plotting the load vector direction versus true horizontal. The stator load angles matched the theoretical values (i.e. 0° for the #2-3-4 axis) to within a few degrees.

POWER CHARACTERIZATION

POWER CONSUMPTION OF SINGLE CORE

The power required by the bearing C-cores as a function of magnetic force, current, temperature, and speed was also determined. At R.T., the average resistance (R) for a C-core (2 coils) is 0.48 ohms and inductance (L) is 18 mH. The real power used by the C-core is a function of the output voltage of the pulse width modulation amplifier (22 kHz switching frequency) and the instantaneous current. Figure 17 shows the typical power system for one C-core.

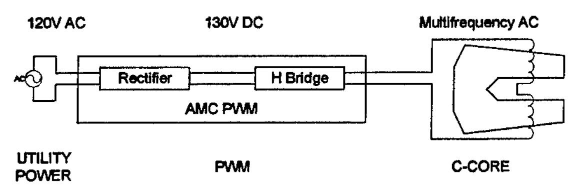

Figure 17 – Power system for one C-Core.

The high switching frequency (22 kHz) of the PWM amplifier makes it difficult to measure the power required to produce bearing forces. Normal 60 cycle RMS power measurements cannot be applied. A high-speed scope (1 million samples/sec) was used to record the instantaneous voltage across the coil as well the instantaneous current through the coil. The isolated, high impedance scope collected 10,000 samples (10 ms). Average power for that time was calculated using a power factor equal to zero.

POWER MEASUREMENTS

Average power as a function of temperature was calculated for C-core #2 and the #2-3-4 magnetic axis at zero RPM. The power for the magnetic axis is the sum of the power from the three C-cores in that axis. All the power calculations are shown in Figure 18 and 19.

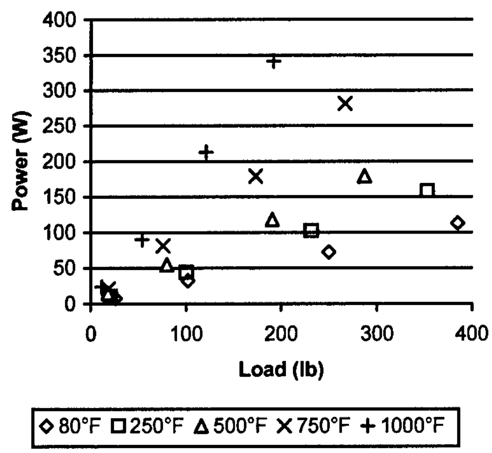

Figure 18 – Power consumption of C-core #2 at zero RPM.

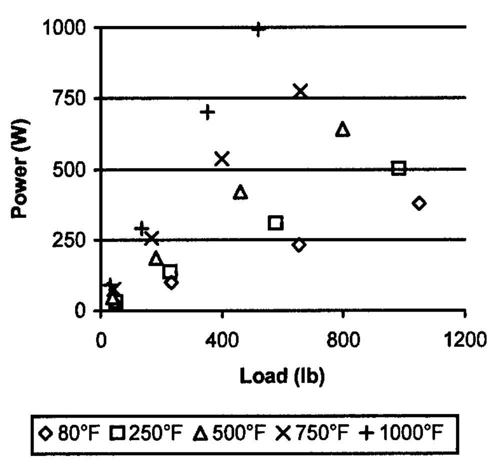

Figure 19 – Power consumption of magnetic axis #2-3-4 at zero RPM.

The largest power requirement was about 1 kW at 1,000 °F (538 °F) to produce 517 lb (2.3 kN) on an axis. Power required to produce a specific load increases dramatically with temperature for a number of reasons. Resistive power losses increase since coil resistance increases. A small degradation of the flux carrying capacity of the Hiperco laminations at temperature also contributes to an increase [3]. The other factor here stems from the increase in the air gap dimension.

THERMAL ANALYSIS

INCREASE IN AIR GAP DUE TO THERMAL EXPANSION

A major contribution to the decrease in load and the increase in power as temperature rises is the expanding gap between the rotor and the stator. Since the heaters are mounted directly on the outside of the stator, it heats at a much higher rate then the rotor, which relies only on convection and radiation for heating. Thus, the rotor will not have expanded as much as the stator, and as a result, the gap will be larger than nominal.

In hindsight, it would seem advantageous to heat the rotor as well as the stator to alleviate thermal mismatch problems. With the current rig setup, however, this is not possible. Stresses generated from thermal expansion of the zero clearance bearing sleeves might cause the ball bearings to seize. In addition, the grease used to lubricate these bearings is only rated to 275 °F (135 °C). In a future build, the ball bearings will be replaced with high temperature, hydrostatic bearings to allow for consideration of other heating methods and allow for testing at higher speeds, since the ball bearings heat up within minutes to their temperature limits.

In order to better understand the growth of the gap, a linear thermal expansion analysis was conducted. The gap at any temperature has a minimum and maximum value just due to the tolerance stack up of the rotor and stator bearing components. The actual gap, which is somewhere between the max and min, will change with thermal mismatch. Thermal maps of the magnetic bearing section of the rotor were generated using temperatures measured

at several different points on the rig using a handheld infrared thermometer. Figure 20 shows that, even after 2.5 hours, the average gap dimension is greater than it is at room temperature. It is quite possible that the rotor would never reach 1,000 °F (538 °C) using the current heating method. The thermal map in Fig. 21 shows a temperature gradient on the rotor. This was due to different heating rates of each of the three band heaters (bands not in 100% contact with stator) and also because the outer containment shell was removed for these tests allowing for convective cooling of the duplex ball bearing. Figure 22 shows that the rotor did reach a uniform temperature of about 780 °F (415 °C) after 2.5 hours of steady heating once the stator poles reached 1,000 °F (538 °C).

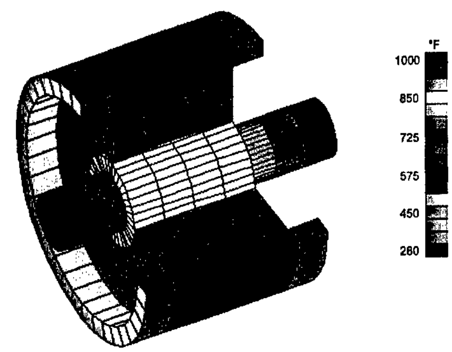

Figure 22 - Thermal map of rotor and stator after rig at 1000 °F for two hours

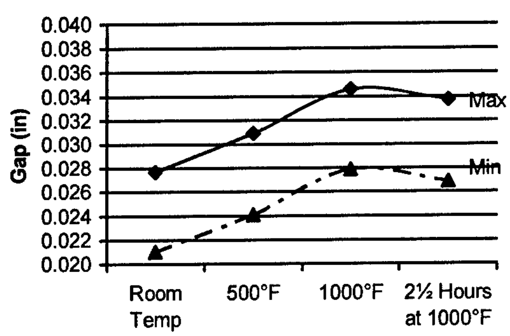

Figure 20 – Theoretical gap between stator and rotor as a function of temperature using linear method.

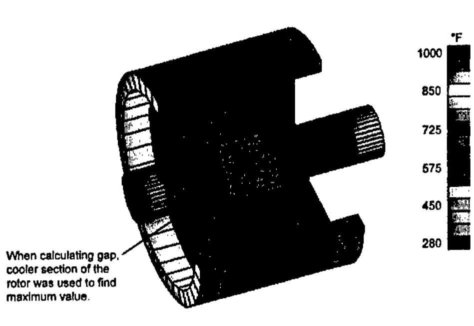

Figure 21 – Thermal map of rotor and stator when rig first reaches 1000 °F

In this model, the average radial gap at room temperature is 0.0244 in. (0.620 mm). This gap increases to 0.0312 in. (0.792 mm) at 1,000 °F (538 °C). Since the magnetic force is a function of the inverse square of the distance, it is clear why the force at elevated temperature drops more severely than shown in [7] for a fixed supply current.

THEORETICAL FORCE PREDICTION

For a general magnetic actuator, the force produced by the magnetic flux in the air gap of area A_g is given by:

$$F = \frac{1}{2}\alpha\mu_o A_g \left[\frac{NI}{2G + \frac{L_{iron}}{\mu_r}}\right]^2 \quad (1)$$

In this equation, u_o is the magnetic permeability of free space and NI is the ampere-turns of the coil(s) driving flux through the circuit. 2G represents the total effective magnetic air gap and α is a force de-rating factor, which accounts for leakage, fringing, non-uniformity in flux density across the pole face and finite path permeability [9]. L_{iron} represents the average iron path component of the C-core circuit; u_r is the relative permeability of the iron laminations.

The actuator measurements in this paper are based on the performance of a complete C-core circuit. Therefore, the forced produced by a single C-core is almost twice that obtained using Equation 1, since there are two air gaps between it and the rotor. Each of the two C-core poles is 15° off axis, therefore, the force produced by a single C-core is 1.93 times that obtained using Eq. 1.

Using α = 0.8, $u_o = 4\pi x 10^{-7}$ N/A^2, N = 52*2 turns, A_g = 2.0 in^2 (12.9 cm^2), G = 0.022 in (0.559 mm), L_{iron} = 5.7 in (145 mm), u_r = 500.

Figure 23 shows a comparison between the predicted force using the maximum gaps from the thermal analysis and the actual loads versus the measured current.

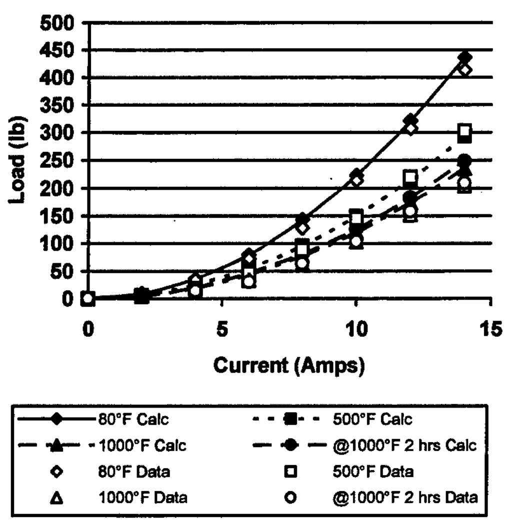

Figure 23 – Theoretical force prediction versus actual measured values for C-core #1

There is good agreement between the calculated load and the actual measurements when the variation in gap is considered.

CONCLUDING REMARKS

Magnetic applied force and electric power for a high load, high speed, high temperature radial magnetic bearing for turbomachinery was measured. Even though the shaft is not doing any work and the rotor is not levitated, these tests provide baseline industry performance characteristics for actual hardware. Load capacity and power consumption of both a single C-core and a magnetic axis were measured from 80 °F (27 °C) to 538 °C. Thermal analysis of the facility to investigate gap growth due to non-uniform heating was performed. Theoretical force predictions were compared to actual results with good correlation. No appreciable decrease in static force production capability was observed due to rotation up to 15,000 rpm at any temperature.

These initial results suggest that the reduction in static force capacity at 1000 °F (538 °F) due to lamination material properties may not be significant. This work also gives practical insight into the range in force capacity that can occur in actual hardware if changes in the rotor-stator gap due to misalignment or thermal effects are not addressed. These factors and the stator mounting technique have to be considered in designing magnetic bearings for high temperature applications.

Future work will include high temperature, high-speed levitation tests without the use of rolling element bearings and high temperature force measurements of a magnetic thrust bearing.

REFERENCES

1) Xu, L., Wang, L., and Schweitzer, G., "Development of Magnetic Bearings for High Temperature Suspension," Seventh International Symp. on Magnetic Bearings, ETH Zurich, August 23–25, 2000.
2) Ohsawa, M., Yoshiolo, K., Ninomiya, H., et al., "High Temperature Blower for a Molten Carbonate Fuel Cell Supported by Magnetic Bearings," 1998, Proceedings of the 6th ISMB.
3) Kueser, P., et al., "Properties of Magnetic Materials for Use in High-Temperature Space Power Systems," NASA SP–3043, 1967.
4) Kondoleon, A., Kelleher, W., "Soft Magnetic Alloys for High Temperature Radial Magnetic Bearings," 7th Inter. Symp. On Magnetic Bearings, pp. 111–116, ETH Zurich, Switzerland, August 23–25, 2000.
5) Mekhiche, M., Nichols, S., Oleksy, J., Young, J., Kiley, J., Havenhill, D., "50K RPM, 1100 °F Magnetic Bearings for Jet Turbine Engines," Seventh International Symp. on Magnetic Bearings, ETH Zurich, Switzerland, August 23–25, 2000.

6) Montague, G.T., Jansen, M.J., Provenza, A.P., Jansen, R.H., Ebihara, B., Palazzolo, A., "Room Temperature Characterization of a Magnetic Bearing for Turbomachinery," NASA/TM—2002-211904, Sept, 2002.
7) Minihan, T., Palazzolo, A., Provenza, A., Montague, G.T., Kascak, A.F., "Fail Safe, High Temperature Magnetic Bearings," IGTI ASME Turbo Expo, Amsterdam June 3–6, 2002.
8) Jansen, R.H., Ebihara, B.E., Montague, G.T., Provenza, A.J., Jansen, M.J., Palazzolo, A., Tucker, R., Preuss, J., Hunt, A., "Design and Construction of a High Temperature, High Load Radial Magnetic Bearing for Turbomachinery," NASA TM to be published, 2002.
9) *Introduction to Magnetic Bearings*, University of Virginia Short Course, presented at the Third International Symposium on Magnetic Bearings, Alexandria, Virginia, 1993.

REPORT DOCUMENTATION PAGE

Form Approved
OMB No. 0704-0188

1. AGENCY USE ONLY *(Leave blank)*

2. REPORT DATE
March 2003

3. REPORT TYPE AND DATES COVERED
Technical Memorandum

4. TITLE AND SUBTITLE
Experimental High Temperature Characterization of a Magnetic Bearing for Turbomachinery

5. FUNDING NUMBERS
WBS–22–708–28–12
1L161102AF20

6. AUTHOR(S)
Gerald Montague, Mark Jansen, Andrew Provenza, Alan Palazzolo, Ralph Jansen, and Ben Ebihara

7. PERFORMING ORGANIZATION NAME(S) AND ADDRESS(ES)
National Aeronautics and Space Administration
John H. Glenn Research Center at Lewis Field
Cleveland, Ohio 44135–3191

8. PERFORMING ORGANIZATION REPORT NUMBER
E–13784

9. SPONSORING/MONITORING AGENCY NAME(S) AND ADDRESS(ES)
National Aeronautics and Space Administration
Washington, DC 20546–0001
and
U.S. Army Research Laboratory
Adelphi, Maryland 20783–1145

10. SPONSORING/MONITORING AGENCY REPORT NUMBER
NASA TM—2003-212183
ARL–TR–2929

11. SUPPLEMENTARY NOTES
Prepared for the 59th Annual Forum and Technology Display sponsored by the American Helicopter Society, Phoenix, Arizona, May 6–8, 2003. Gerald Montague, U.S. Army Research Laboratory, NASA Glenn Research Center; Mark Jansen, Ralph Jansen, and Ben Ebihara, University of Toledo, Toledo, Ohio 43606; Andrew Provenza, NASA Glenn Research Center; and Alan Palazzolo, Texas A&M University, College Station, Texas 77843. Responsible person, Gerald Montague, organization code 0300, 216–433–6252.

12a. DISTRIBUTION/AVAILABILITY STATEMENT
Unclassified - Unlimited
Subject Categories: 07 and 37 Distribution: Nonstandard
Available electronically at http://gltrs.grc.nasa.gov
This publication is available from the NASA Center for AeroSpace Information, 301–621–0390.

12b. DISTRIBUTION CODE

13. ABSTRACT ***(Maximum 200 words)***

Open loop, experimental force and power measurements of a radial, redundant-axis, magnetic bearing at temperatures to 1000 °F (538 °C) and rotor speeds to 15 000 RPM along with theoretical temperature and force models are presented in this paper. The experimentally measured force produced by a single C-core using 22A was 600 lb. (2.67 kN) at room temperature and 380 lb. (1.69 kN) at 1000 °F (538 °C). These values were compared with force predictions based on a 1D magnetic circuit analysis and a thermal analysis of gap growth as a function of temperature. Tests under rotating conditions showed that rotor speed has a negligible effect on the bearing's load capacity. One C-core required approximately 340 W of power to generate 190 lb. (8.45 kN) of magnetic force at 1000 °F (538 °C); however the magnetic air gap was much larger than at room temperature. The data presented is after the bearing had already operated six thermal cycles and eleven total (not consecutive) hours at 1000 °F (538 °C).

14. SUBJECT TERMS
Turbomachinery; Magnetic bearing; C-core; Power factor

15. NUMBER OF PAGES
18

16. PRICE CODE

17. SECURITY CLASSIFICATION OF REPORT	18. SECURITY CLASSIFICATION OF THIS PAGE	19. SECURITY CLASSIFICATION OF ABSTRACT	20. LIMITATION OF ABSTRACT
Unclassified	Unclassified	Unclassified	